Meteoritics & Planetary Science 37, xxx–xxx (2002)
Available online at http://www.uark.edu/meteor

An entry model for the Tagish Lake fireball using seismic, satellite and infrasound records

PETER G. BROWN[1]*, DOUGLAS O. REVELLE[2], EDWARD TAGLIAFERRI[3] AND ALAN R. HILDEBRAND[4]

[1]Department of Physics and Astronomy, University of Western Ontario, London, Ontario N6A 3K7, Canada
[2]Los Alamos National Laboratory, P.O. Box 1663, Los Alamos, New Mexico 87545, USA
[3]ET Space Systems, 5990 Worth Way, Camarillo, California 93012, USA
[4]Department of Geology and Geophysics, University of Calgary, Calgary, Alberta T2N 1N4, Canada
*Correspondence author's e-mail address: pbrown@uwo.ca

(Received 2001 December 17; accepted in revised form 2002 April 10)
(Part of a series of papers on the Tagish Lake meteorite)

Abstract–We present instrumental observations of the Tagish Lake fireball and interpret the observed characteristics in the context of two different models of ablation. From these models we estimate the pre-atmospheric mass of the Tagish Lake meteoroid to be ~56 tonnes and its porosity to be between 37 and 58%, with the lowest part of this range most probable. These models further suggest that some 1300 kg of gram-sized or larger Tagish Lake material survived ablation to reach the Earth's surface, representing an ablation loss of 97% for the fireball. Satellite recordings of the Tagish Lake fireball indicate that 1.1×10^{12} J of optical energy were emitted by the fireball during the last 4 s of its flight. The fraction of the total kinetic energy converted to light in the satellite pass band is found to be 16%. Infrasonic observations of the airwave associated with the fireball establish a total energy for the event of 1.66 ± 0.70 kT TNT equivalent energy. The fraction of this total energy converted to acoustic signal energy is found to be between 0.10 and 0.23%. Examination of the seismic recordings of the airwave from Tagish Lake have established that the acoustic energy near the sub-terminal point is converted to seismic body waves in the upper-most portion of the Earth's crust. The acoustic energy to seismic energy coupling efficiency is found to be near 10^{-6} for the Tagish Lake fireball. The resulting energy estimate is near 1.7 kT, corresponding to a meteoroid 4 m in diameter. The seismic record indicates extensive, nearly continuous fragmentation of the body over the height intervals from 50 to 32 km. Seismic and infrasound energy estimates are in close agreement with the pre-atmospheric mass of 56 tonnes established from the modeling. The observed flight characteristics of the Tagish Lake fireball indicate that the bulk compressive strength of the pre-atmospheric Tagish Lake meteoroid was near 0.25 MPa, while the material compressive strength (most appropriate to the recovered meteorites) was closer to 0.7 MPa. These are much lower than values found for fireballs of ordinary chondritic composition. The behavior of the Tagish Lake fireball suggests that it represents the lowest end of the strength spectrum of carbonaceous chondrites or the high end of cometary meteoroids. The bulk density and porosity results for the Tagish Lake meteoroid suggest that the low bulk densities measured for some small primitive bodies in the solar system may reflect physical structure dominated by microporosity rather than macroporosity and rubble-pile assemblages.

INTRODUCTION

Meteoric fireballs accompanying the fall of a meteorite are spectacular events, often noted by thousands of eyewitnesses. Unfortunately, the short duration of such an event and its relative rarity make more detailed recordings of these events scarce. Camera networks established in Canada (Halliday *et al.*, 1978), the U. S. (McCrosky and Boeschenstein, 1965) and in Europe (Oberst *et al.*, 1998) have collectively recorded detailed photographic records associated with three meteorite falls (Pribram, Innisfree and Lost City). These records provide a unique bridge between the dynamical behavior of the larger meteoroid parent objects in the atmosphere with recovered meteorites. Such records are valuable for establishing gross physical characteristics of the original body (such as compressional strength, bulk density and porosity) as well as

Prelude preprint MS#4709
© Meteoritical Society, 2002. Printed in USA.

establishing pre-atmospheric mass and orbits. These data represent a means of "probing" the physical structure of small asteroidal (about a few meters in diameter) bodies.

At present only one fireball camera network continues to operate (the European Network), though fortuitous video recordings of two recent meteorite falls have further expanded the suite of orbital and physical properties available for the pre-atmospheric meteoroids associated with such falls (Brown *et al.*, 1994; Borovica *et al.*, 2002, unpubl. data). In all five cases, the meteorites which have these ancillary dynamical data associated with their fireballs have been ordinary chondrites.

More recently, global observations by U. S. Department of Defence satellites (Tagliaferri *et al.*, 1994) have proven useful in recording some fireball characteristics (such as total radiated energy and trajectory information) for brighter events. These data together with supplementary instrumental recordings on the ground now permit (in principle) much better characterization of most large meteorite falls.

In particular, instrumental detections of the airwave associated with fireballs have been used in the past as a means to establish trajectory and approximate energy estimations (cf., Qamar, 1995) for individual events. Such data have, however, not been available for meteorite-producing fireballs with well-determined trajectories and velocities. These data taken together would allow measurement of the energy, pre-atmospheric radius, fragmentation behavior and porosity of the body to be constrained. Furthermore, the fraction of the total energy converted to acoustic wave energy and a better understanding of the poorly understood mechanism of coupling of the acoustic wave to the ground might be better determined.

At 16:43 U.T. (08:43 A.M. local time) on 2000 January 18, a bright fireball was observed over Alaska, the Yukon, and northern British Columbia (Canada). The event was witnessed as far away as 700 km from the terminal point and the accompanying detonations were detectable for at least several hundred kilometers. This fireball was associated with the fall of the Tagish Lake meteorite, an unusual carbonaceous chondrite (Brown *et al.*, 2000). The airwave signal from the fireball was recorded on three local seismic stations, Whitehorse (WHY), Haines Junction (HYT) and Dease Lake (DLBC). The airwave was detected directly as well by several more distant infrasound detectors in Wyoming, USA and Manitoba, Canada.

The Tagish Lake meteoroid was also observed by satellites operated by the U. S. Department of Defence. These data established the atmospheric path for the fireball (when combined with ground-based records; see Hildebrand *et al.*, 2002, for details), an energy based on the optical radiation from the event and a velocity. When combined with the seismic and infrasound records, this has allowed a detailed reconstruction of the fragmentation behavior, the bulk compressive strength and size of the pre-atmospheric Tagish Lake meteoroid.

Examining these results in the context of two numerical entry models has allowed us to construct a physical picture of the several meter-sized asteroid which was the original Tagish Lake meteoroid. In addition to this specific physical picture, we compare the dynamical parameters of the Tagish Lake fireball with the population of well-recorded camera network fireballs to attempt to associate ground-truthed physical/ compositional characteristics from this event to the broader fireball population, from which material is not available for examination.

Some of this analysis draws on accompanying results presented in Hildebrand *et al.* (2002).

GROSS FRAGMENTATION ENTRY MODEL OF TAGISH LAKE AND INITIAL MASS

One measure of the initial mass of the Tagish Lake meteoroid may be made by modeling its energy release as recorded by satellite systems. Figure 1 is the light curve associated with the fireball recorded by U. S. Department of Defence satellites which record the light flashes produced by sufficiently large bolides. The fireball was detected for 2 s in the silicon pass band (400–1100 nm wavelength). Assuming the fireball radiates as a 6000 K blackbody, the integrated optical light energy from the fireball is 1.1×10^{12} J; this most energetic fraction of the fireball's duration is reasonably assumed to represent most of the kinetic energy dissipated by the meteoroid during its deceleration. A discussion of the sensors and techniques for processing these optical satellite data as well as the reasoning and possible uncertainties in assuming a 6000 K blackbody model are discussed in Brown *et al.* (1996) and Tagliaferri *et al.* (1994).

The results of the St-Robert fireball/meteorite fall (Brown *et al.*, 1996; Hildebrand *et al.*, 1997) having both cosmogenic nuclide activities from recovered meteorites (which constrained the entry mass (Leya *et al.*, 2001)) and satellite data available, yield an apparent integral luminous efficiency (τ_i) of ~10% in the silicon pass band of the satellite sensor for this H chondrite. This corresponds to the fraction of the total initial kinetic energy converted to radiation in this pass band.

Adopting this conversion efficiency as well as the integrated optical energy and the initial velocity (15.8 km/s) determined from Hildebrand *et al.* (2002) (hereafter H2002) we derive an initial mass estimate near 9×10^4 kg for Tagish Lake. Given the unusual makeup of Tagish Lake as compared to H chondrites, we may anticipate that the true efficiency will be somewhat different. Taking the range of physically probable integral efficiencies to be from 5 to 20%, implies probable mass ranges from 5×10^4 to 1.8×10^5 kg.

To better estimate the initial mass, we use the simple entry model employed to interpret the light curve and initial mass for the St-Robert fireball (Brown *et al.*, 1996), namely that of the gross fragmentation model of Ceplecha *et al.* (1993). The adopted entry angle, initial velocity and heights of initial break-up from H2002 are shown in Table 1. Together with the satellite observed light curve these dynamical data provide the necessary constraints for the modelling. Our goal is to

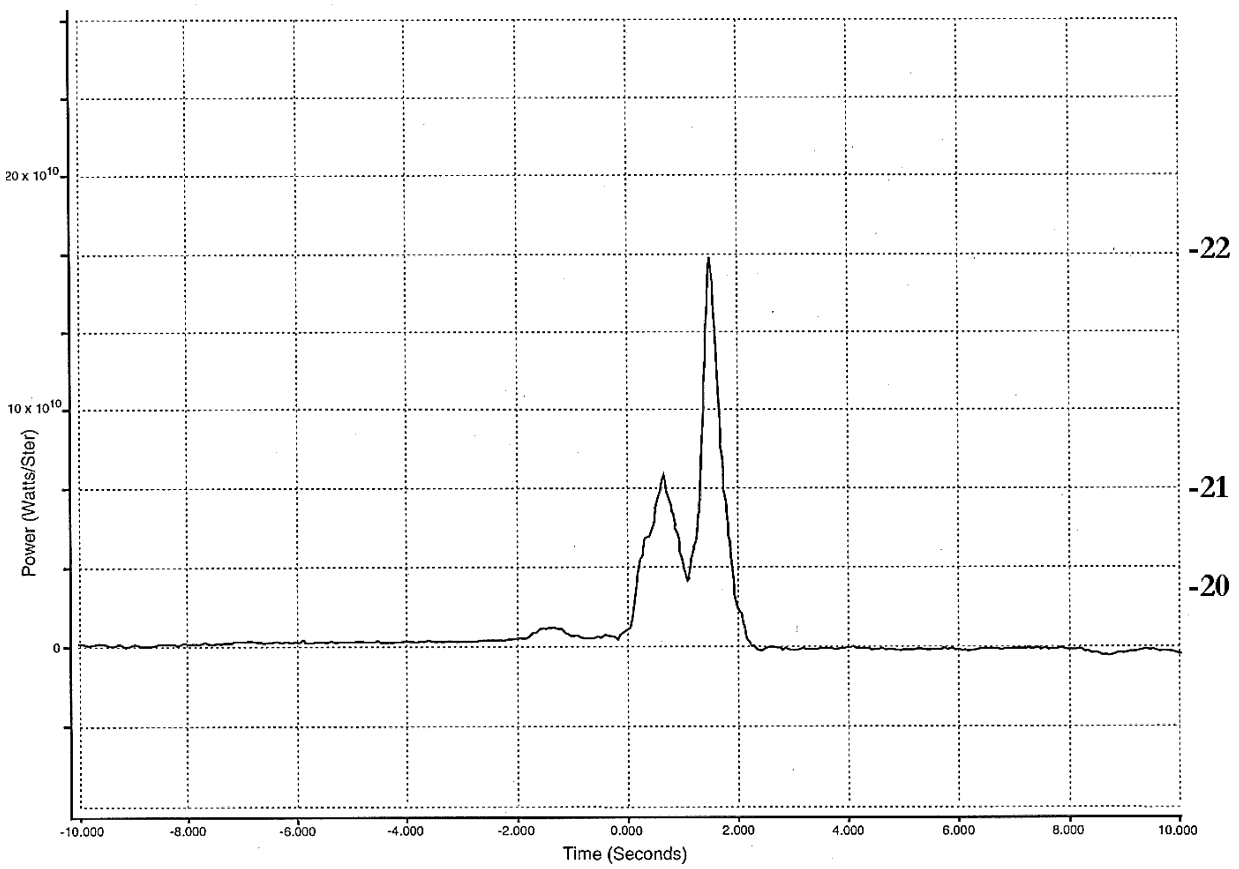

FIG. 1. Satellite optical light curve of the Tagish Lake fireball. The left ordinate shows radiated power from the fireball in units of Watts/steradian and the right ordinate is a measure of the equivalent absolute visual magnitude assuming Tagish Lake emits as a 6000 K blackbody. The abscissa is in units of seconds references to an origin of 16:43:43 U.T. 2000 January 18.

TABLE 1. Computed trajectory, velocity and fragmentation height for the Tagish Lake fireball based on various data sets summarized from Hildebrand *et al.* (2002).*

Initial velocity (km/s)	15.8 ± 0.6
Radiant azimuth (°)	330.7
Radiant altitude (°)	17.8
Height of earliest fragmentation (km)	48
Height of beginning of major fragmentation (km)	37
End height (km)	29

*The azimuth and altitude refer to the apparent local radiant azimuth and altitude as seen from the terminal ground point.

determine the initial mass assuming a constant ablation coefficient. We note that the light so-produced is referenced to the panchromatic, velocity-dependent luminous efficiency scale as revised by Ceplecha (1996) who, from analysis of the Lost City meteorite fall, found a value for the differential luminous efficiency of $\tau_d = 6.1\%$ at 13 km/s. This represents the instantaneous fraction of kinetic energy converted to light. The output from this model in units of equivalent visual stellar magnitudes can then be directly compared to the satellite data in the silicon pass band assuming a 6000 K blackbody emission for the bolide.

We expect that for such a fragile body the value for the ablation coefficient (σ) will be larger than chondritic values and most likely in the range 0.04–0.20 $s^2\ km^{-2}$. The implication of this larger σ is that the effective luminous efficiency will be higher than the chondritic value (cf., ReVelle, 1983) and that estimates from this simple model are upper limits (within the constraints of an assumed constant ablation coefficient).

Specifically, we take $\sigma = 0.02\ s^2\ km^{-2}$ and a shape-density coefficient, K, (with $K = \Gamma A m^{-0.66}$, where Γ is the assumed drag coefficient, A is the cross sectional area and m is the mass) of 0.46 (Ceplecha *et al.*, 1998) as appropriate for chondritic bodies to compute an upper limit for the initial mass of 115 tonnes. This is the equivalent mass of an ordinary chondrite needed to emulate the dynamics and observed light curve of Tagish Lake.

To examine the effects of changing σ (particularly to expected higher values), we use the mean value for type II fireballs (which are believed to be associated with carbonaceous chondrites) as given in Ceplecha *et al.* (1998). Here we take $\sigma = 0.042\ s^2\ km^{-2}$ and $K = 0.69$ to again fit the light curve.

This produces a mass estimate of 97 tonnes, which should be taken as an upper limit to the true mass. Extending this to higher σ makes matching the light curve and dynamical parameters effectively impossible. This is due to our adopted simplification in using a constant ablation coefficient. Our ordinary chondritic fit to the light curve is shown in Fig. 2.

POROSITY MODEL OF TAGISH LAKE

We now apply a more general ablation model which takes into account variable σ and incorporates porosity explicitly in an effort to derive a more accurate initial mass. This is a recent adaptation (ReVelle, 2001) of an earlier proposed model (ReVelle, 1983) which incorporates the porosity of the ablating body directly in the equations of motion. This model assumes an ordinary chondritic-like composition while complementarily varying porosity and density. In this ablation model, increased porosity increases heat transfer between the airstream and the body which in turn leads to an increased ablation coefficient (σ) and higher end heights, all other parameters being equal. As shown by ReVelle (2001), the visible light production per unit mass is also much higher for higher porosity bodies. This model explains the end-height differences of different classes of fireballs identified by Ceplecha and McCrosky (1976) as being due to differing bulk densities/porosities. Different classes of fireballs are expected to have somewhat different compositions.

In terms of observed dynamics, the porosity and the zero porosity (uniform bulk density or equivalently 0% porosity) models do not differ greatly; thus data using dynamical constraints alone will not distinguish between the models. However, the order of magnitude light production predicted for the Tagish Lake meteoroid by the models implies that detailed light curves may serve as a diagnostic for determination of porosity in the general case. As well, the porosity model generally has much higher ablation rates than the zero porosity model.

The porosity model permits explicit breakup of a body once a preset compressive strength is exceeded so that a variable number of resulting fragments is produced. Each of these fragments will again fragment in a hierarchical manner when their crushing strength is exceeded and so forth. The combined light production from each fragment collectively produces the final light curve. The physical underpinnings of this model and its details can be found in ReVelle (1983, 1993, 2001).

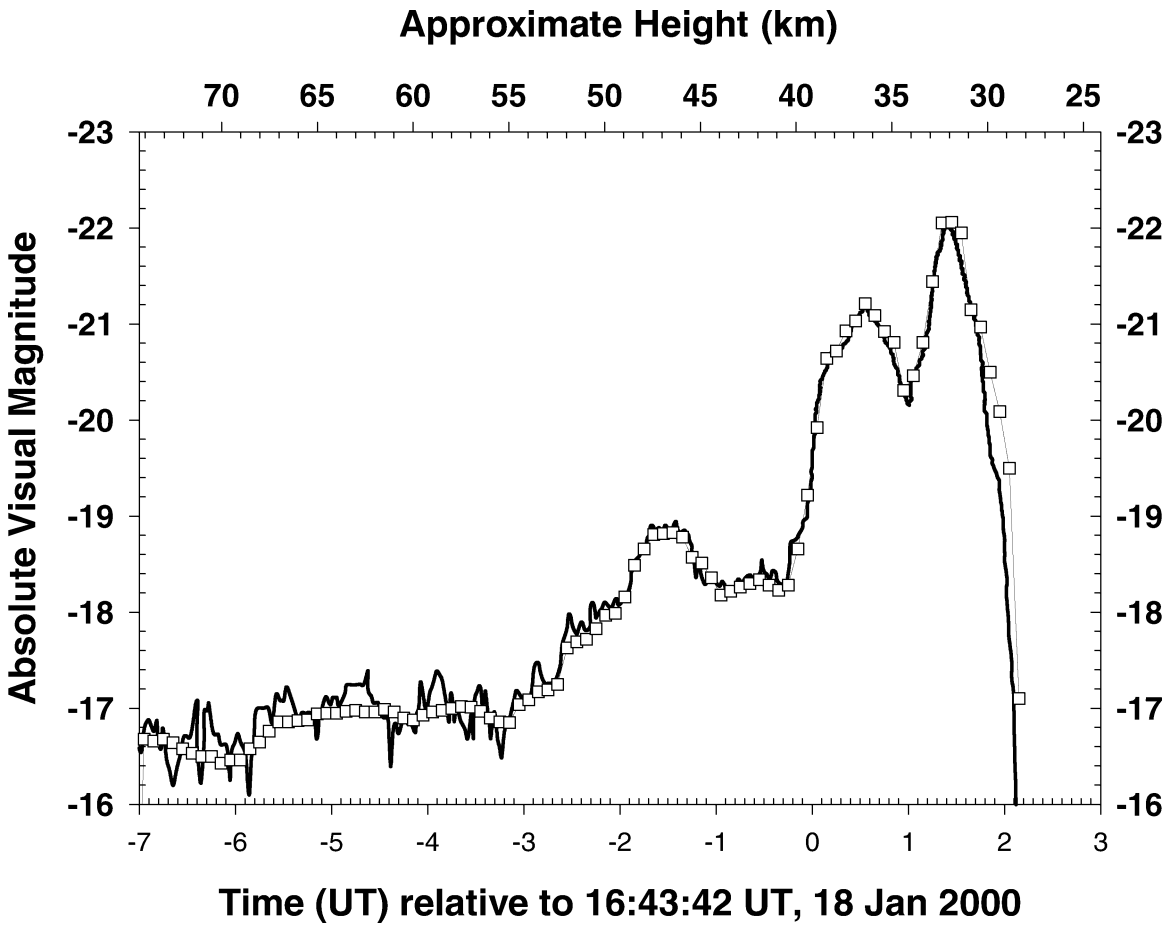

FIG. 2. Observed *vs.* theoretical light curve using the gross-fragmentation model for the Tagish Lake fireball. The solid line is the satellite observed light curve of the fireball, open squares are model fits. Details are given in the text.

We add a cautionary note in the interpretation of the results that follow: these are not unique answers; however, a limited range of allowable combinations of number of fragments, initial porosity and initial radius, results from the dynamical constraints available for Tagish Lake (velocity, end height, entry angle) combined with the light curve. The match to the dynamical and light curve constraints is produced through forward modelling within the context of the assumed number of fragments and when fragmentation is observed to begin.

The Tagish Lake modeling results are given in Table 2. Note that the general porosity model (bottom of Table 2) provides a best fit with the satellite light curve for an initial mass of 56 tonnes and (using the measured mineral grain density of Tagish Lake, from H2002) a porosity of 37%. Figure 3 shows the variation in mass, velocity, ablation coefficient and ram pressure as a function of height for this model run. Predicted end heights without fragmentation are up to 10 km lower than shown in Table 2. Variations in the assumed compressive strength by factors of 2 to 3 (which affects the height of initial breakup) may change the modelled end height by as much as 5 km.

These model results were obtained assuming a spherical meteoroid (shape-factor $S_f = Am^{-0.66}\rho^{0.66} = 1.209$), with initial radius of 2 m, initial velocity at entry of $V_\infty = 15.8$ km/s, entry angle (θ) of 18°, and imposing the additional constraint that only 1% of the initial kinetic energy is remaining at the end height/luminosity-cutoff (as has been found for the three photographically recorded meteorite falls; cf., ReVelle, 1979). Additionally, we assume break-up into 10 fragments once the ram pressure exceeds the compressive strength of the body and after an initial short-time interval, these fragments are advected into the wake, heat-up and subsequently radiate light. Fragments were assumed in these runs to act collectively after this advection delay so that the frontal area was increased compared to the size of the individually broken and still ablating fragments. The atmosphere used in the model was assumed to be an isothermal, hydrostatic atmosphere. The porosity values are given for a mineral grain density of 2.65 g cm^{-3} as measured for individual Tagish lake fragments (see H2002). The observed end height was near 29 km and the end velocity was measured to be near 9 km s^{-1} (H2002). The zero porosity model uses the physical ablation characteristics of the average fireball in each of the fireball groups described in Ceplecha *et al.* (1998) to allow comparison with the nominal results for Tagish Lake. Additionally, we define a group 0 which corresponds to the physical makeup expected of an iron meteoroid.

As can be seen from Table 2, slightly higher porosity and lower initial masses are also moderate matches to the lightcurve and dynamics, with values up to 58% porosity and initial masses as low as 37 tonnes providing acceptable fits. The upper portion of the table shows the results for the same model, but assuming 0% porosity (the zero porosity or uniform bulk density model) using the input parameters appropriate to each of the observed fireball groups of Ceplecha and McCrosky (1976). None of the uniform bulk density model runs were able to reproduce both the observed dynamics and light curve. Our best-fit porosity (37%) result suggests ~1300 kg of gram-sized and larger fragments survived to the end of ablation to fall to the ground as meteorites.

INFRASOUND RECORDINGS

The airwave from the Tagish Lake fireball was detected infrasonically by the IS10 infrasound station of the International Monitoring System, located at Lac du Bonnet, Manitoba, Canada (50°12' N, 96°1' W). Additionally, a marginal detection

TABLE 2. Porosity modeling results for Tagish Lake (see text for explanation).

	End height (km)	Speed (km/s)	Initial mass (kg)	Surviving mass (kg)	Light curve match (Y/N)
Zero porosity modeling					
Group O.-Fe	9.78	11.77	2.61×10^5	2.99×10^4	N
Group I	15.08	4.40	1.24×10^5	1.38×10^4	N
Group II	23.44	8.57	7.04×10^4	1.09×10^4	N
Group IIIA	36.42	12.80	2.51×10^4	7.80×10^3	N
Group IIIB	47.72	14.38	9.05×10^3	4.91×10^3	N
Tagish Lake: $\rho_m = 1600$ kg/m^3	25.64	9.29	5.52×10^4	8.98×10^3	N
Porous modeling:					
Bulk density porosity (g cm^{-3})					
2.59 2%	21.02	6.41	8.68×10^4	5.55×10^3	N
2.22 16%	23.59	7.40	7.44×10^4	3.49×10^3	N
1.85 30%	26.62	8.57	6.20×10^4	1.96×10^3	N
1.67 37%	28.07	9.22	5.58×10^4	1.33×10^3	Y (Very good)
1.48 44%	29.65	9.89	4.96×10^4	8.60×10^2	Y(Good)
1.30 51%	31.71	10.60	4.34×10^4	5.51×10^2	Y
1.11 58%	34.03	11.32	3.72×10^4	3.57×10^2	Y

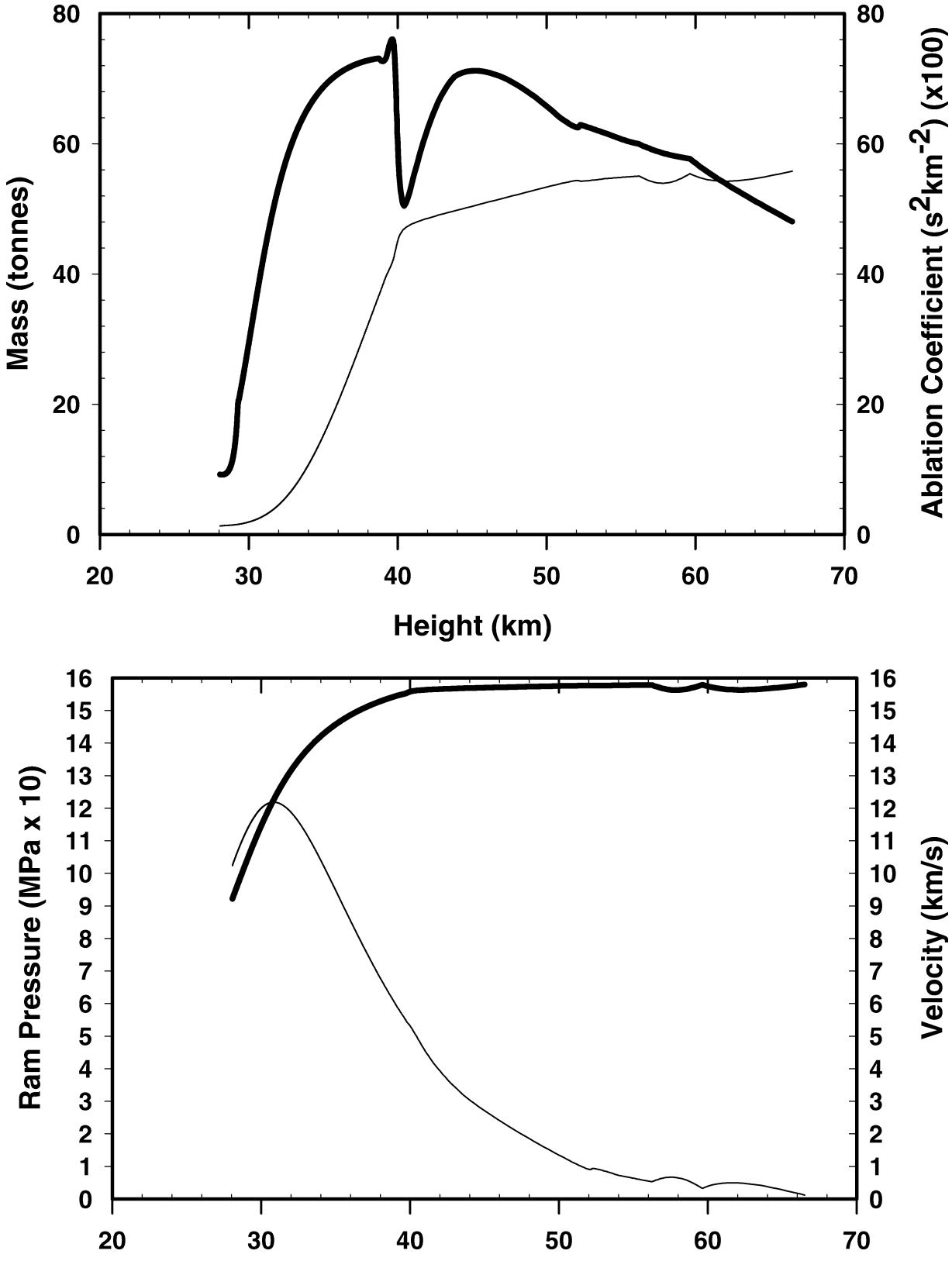

FIG. 3. Theoretical meteoroid/fireball parameters as determined through application of the porosity model. The top graph shows the mass as a function of height (thin line) and the ablation coefficient (thick line). The bottom plot shows the velocity *vs.* height (thick line) and the instantaneous forward ram pressure on the meteoroid (thin line). These values are appropriate to a meteoroid with 37% porosity and 56 tonne initial mass.

may have occurred at the Pinedale infrasound station in Wyoming, but instrumental noise does not allow certain association of several possible signals with the fireball.

Infrasound refers to that part of the acoustic frequency spectrum which is sub-audible in the high-frequency limit (<20 Hz) and greater than the natural oscillation frequency of the atmosphere (associated with gravity waves) in the low-frequency limit (>0.01 Hz). At lower frequencies in particular, the acoustic energy experiences little attenuation, resulting in detectability over very large propagation distances (cf., ReVelle, 1976, for a review of bolide infrasound).

The IS10 array consists of four widely spaced microphones sensitive to infrasound. By cross-correlating the output from each microphone and performing beamforming of the signals it is possible to determine the arrival azimuth and elevation for a coherent signal (cf., Evers and Haak, 2001). We use the coherence of the signal over the full baseline of the array to distinguish true signals from local noise at each microphone.

The signal associated with the Tagish Lake fireball detection at IS10 is shown in Fig. 4. The raw signal has been band pass filtered between 0.5 and 1.5 Hz to maximize the signal-to-noise ratio. The signal persists for ~10 min as would be expected for a signal dispersed over a range of 2640 km, the distance from IS10 to the Tagish Lake fireball terminal point. The peak-to-peak amplitude of the signal is 24 MPa, which is ~3× the noise background in this band pass at IS10 on this day.

The azimuth of the signal from IS10 is 306° which is very close to the great circle azimuth of 309° between IS10 and the Tagish Lake fireball terminal point. The time delay from the time of the fireball to the onset of the signal (8230 s) yields a mean signal speed of 0.32 km/s which is at the upper end of typical long-distance ducted atmospheric returns (Ceplecha *et al.*, 1998). This is most likely a stratospherically ducted signal and we suggest the high average signal speed is attributable to the very high stratospheric wind speeds present in the direction from Tagish Lake to IS10 (velocities of ~60 m/s).

From these acoustic data, it is possible to derive approximate source energies incorporating a variety of assumptions. These techniques and their limitations are discussed in detail in ReVelle and Whitaker (1999) as well as ReVelle (1976). The most commonly applied technique for infrasonic energy measurements of bolides is the period at maximum amplitude approach (ReVelle, 1997). The signal period tends to be a more robust measure than amplitude, which may be significantly affected by winds and local topography. This period method is based on an empirical relation between the observed period at maximum signal amplitude (P) for stratospheric returns and known yields (E in kilotonnes of TNT; 1 kT = 4.185×10^{12} J) for U. S. nuclear tests (ReVelle, 1980):

$$\log \frac{E}{2} = 3.34 \log(P) - 2.58 \qquad (1)$$

This relation has been applied to a large number of energetic bolide events (ReVelle, 1997) and found to be in reasonable agreement with other independent energy estimates for the same events.

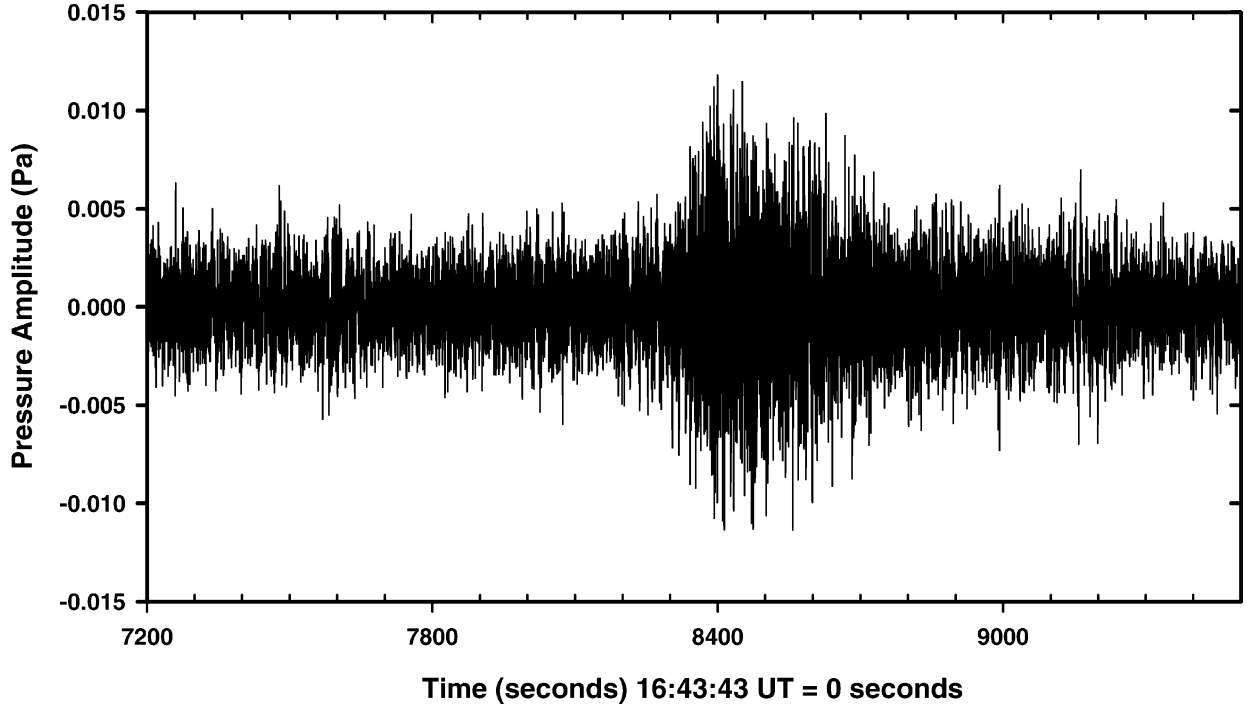

FIG. 4. Infrasonic signal produced by the Tagish Lake fireball as recorded at the IS10 Lac du Bonnet, Manitoba (50°12' N, 96°1' W) infrasound station. The waveform has been bandpassed from 0.5 to 1.5 Hz. The range from IS10 to the terminal burst of the Tagish Lake fireball is 2640 km at a bearing of 309.2° as seen from IS10. The signal arrives from an azimuth of 307°.

For our infrasonic signal, the average signal period from all four channels is 5.6 ± 1.3 s. These measurements are from the zero-crossings for each of the four channels and produced using an average and standard deviation from all four channels. This is the same technique as was used for the signal analysis applied to derive Eq. (1). Using Eq. (1) this corresponds to a yield of 1.66 ± 0.70 kT. This small explosion yield, coupled with the fast, high southeast-directed stratospheric winds probably results in the lack of a detectable signal at several infrasound stations in the southwestern United States. Using an initial velocity of 15.8 km/s (from H2002), this energy yield corresponds to an object of mass 56 tonnes, and using a bulk density of 1.6 g cm^{-3} (H2002), to a pre-atmospheric meteoroid size of just over 2 m in radius.

Taking this energy estimate and its error as a robust representation of the true source energy (which from comparison with the modeling section we see is a good assumption) we may also estimate the acoustic efficiency for the Tagish Lake fireball. This represents the fraction of total initial kinetic energy which is converted into acoustic wave energy (cf., ReVelle and Rajan, 1979). It is the acoustic analog of the more familiar luminous efficiency. In particular, we may sum the total pressure perturbation associated with the signal at IS10 to estimate the total energy at the source *via* (ignoring focusing and reflection effects):

$$\varepsilon_{\rm ac}\left\{\frac{W}{2\pi}\right\}R^{-2} = \int_0^{\tau_d} \frac{\Delta P_{\rm o-p}^2}{\rho c_{\rm s}}\,dt \qquad (2)$$

where t is time, $\tau_{\rm d}$ is acoustic signal duration, $\Delta p_{\rm o-p}$ is the positive signal amplitude ($\sim\Delta p_{\rm p-p}/2$), ρ is the air density at the receiver, $c_{\rm s}$ is the adiabatic sound speed at the observation level, R is the range from the source to the receiver, W is the yield at source and $\varepsilon_{\rm ac}$ is the acoustic efficiency.

Here we use $\rho = 1.225$ kg m^{-3}, $c_{\rm s} = 310$ m/s, $R = 2.64 \times 10^6$ m, $\tau_{\rm d} \approx 600$ s (windowed over the apparent duration of the signal). The final pressure used in the integrand in Eq. (2) has noise subtracted by approximating the mean background noise in windows of identical duration both before and after the signal. Setting W = 1.66 kT (as our period-at-maximum amplitude nominal energy estimate) produces an acoustic efficiency value of 0.13%. For the upper and lower bounds of the energy estimate, we find the possible range of acoustic efficiency to be 0.10–0.23%. For comparison, ReVelle and Whitaker (1997) found acoustic efficiency ranges from 0.2 to 7% from examination of 10 infrasonic bolide events detected at multiple stations. The fact that our values fall at the low end of their range may reflect the atypical composition (and hence ablation behavior) of the Tagish Lake fireball.

SEISMIC DATA

The airwaves generated by the passage of the Tagish Lake meteoroid were detected at three seismic stations. Other work has demonstrated the utility of deriving parameters for bolide trajectories from seismic data alone (cf., Qamar, 1995) when numerous stations detect the airwave. In the present case, however, only two seismic stations showed strong signals from the fireball and one other a weak probable signal. Fortunately, the entry geometry has been well defined from other data (H2002) allowing detailed interpretations from this limited station coverage.

The airwave from a meteoroid can initiate seismic waves in the solid earth in several ways. First, the airwave itself may force transverse oscillations at the Earth's surface due to the overpressure of the wavefront; these we will refer to as air-coupled Rayleigh waves, which may itself consist of several components. Second, the acoustic wave may match the natural seismic wave velocities in the ground and excite these modes directly; these will be referred to as air-coupled body waves, usually P-type seismic (longitudial) waves. Finally, the airwave may be detected as it directly deforms rock proximal to a seismic station.

The seismic station near WHY recorded a large impulsive (and relatively long lasting) signal beginning 208 s after the main detonation recorded at 16:43:43 U.T. Using a high-pass filter on these data (>1 Hz), an apparently related signal begins some 128 s after the main detonation time (Fig. 5). Note that the small event near 400 s (at ~16:50) appears in all regional seismograms and is a teleseismic event (earthquake) unrelated to the fireball.

The strongest arrival at WHY is interpreted as having resulted from the main airwave/audible explosion. This signal apparently records the first direct arrival of the airwave after it propagated in the direction normal to the fireball trajectory as a cylindrical blast wave. Rayleigh waves moving at acoustic velocities in the topmost portion of the ground near the seismic station arrive next. The earliest arrival of the airwave phase is that of an N-wave signature in the vertical component of the seismograph (showing strong downward motion), indicative of that expected of pressure loading of the local terrain (cf., Kanamori *et al.*, 1991). We interpret these as the direct expression of the airwave on the local terrain. The large amplitude of this arrival phase and the Rayleigh waves following it are typical of air-coupled Rayleigh waves which often are the strongest component of seismic records of airblasts due to resonant coupling with unconsolidated surface soil (Ewing *et al.*, 1967).

The earlier P-wave (body wave) arrival is interpreted as resulting from sound coupling near the sub-terminal point of

FIG. 5. *(right)* Seismic records from Haines Junction (HYT) (60°8' N, 137°5' W) (top) and Whitehorse (WHY) (60°7' N, 134°9' W). These seismic records have been corrected for the individual seismograph response function (to produce true ground motion) and high ban passed above 1 Hz. The onset of P-waves are visible at both HYT and WHY beginning near 180 s and WHY shows a clear acoustic/air-coupled rayleigh wave signal starting just after 200 s. The origin time for both stations is 16:43:43 U.T. 2000 January 18.

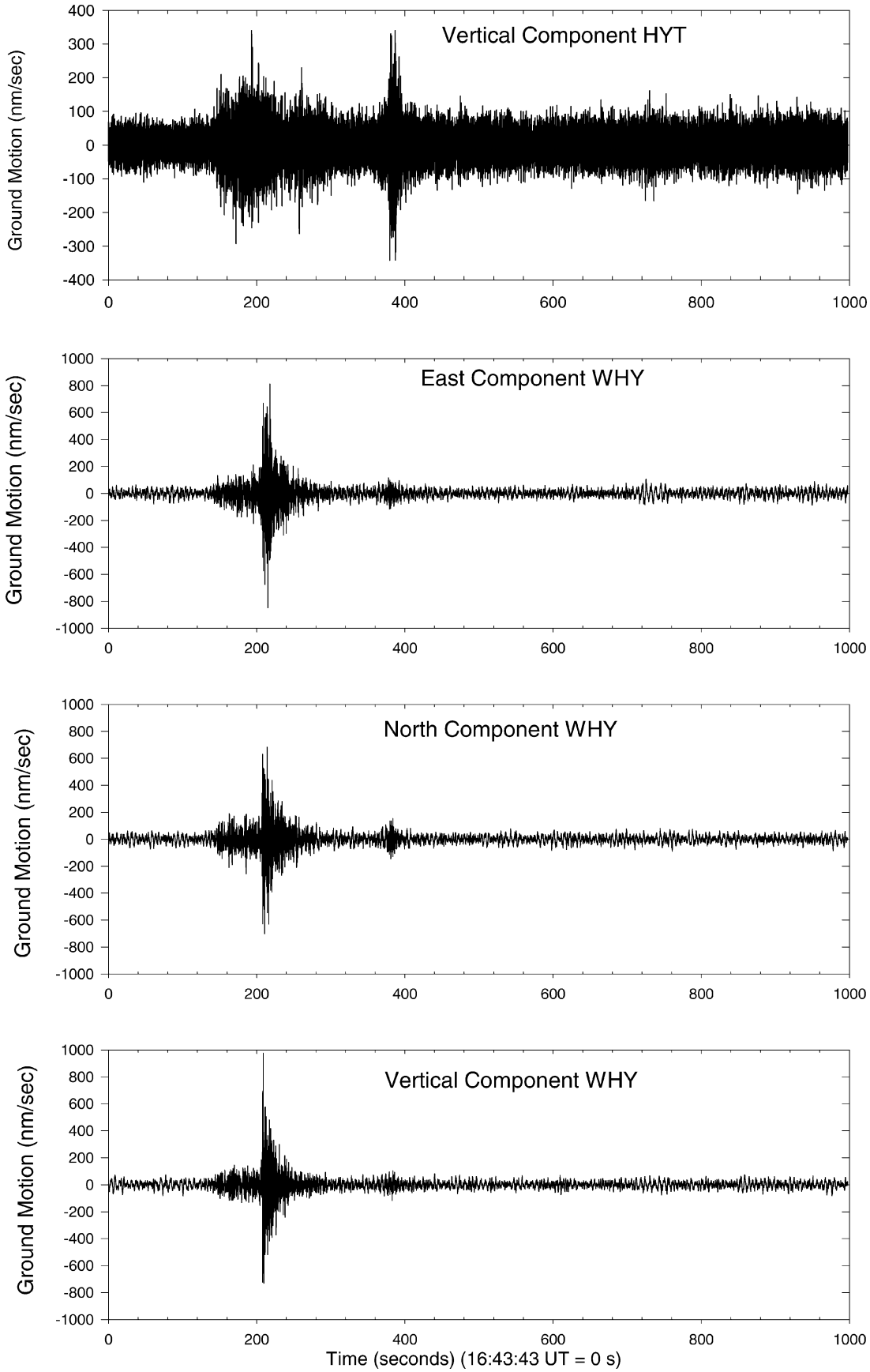
Vertical Component HYT
East Component WHY
North Component WHY
Vertical Component WHY
Ground Motion (nm/sec)
Time (seconds) (16:43:43 UT = 0 s)

the fireball, where the sound first reaches the ground. Provided the amplitude of the blast is sufficient, we expect the shock to couple directly into the ground very near the locus of points directly under the trajectory where the trace velocity across the ground of the cylindrical blast wave is comparable to the local P-wave velocity (assumed as 6 km s^{-1}). Thus, the earliest P-wave signal should be from the region nearest the terminal portion of the fireball trajectory where a significant blast wave is still produced and which reaches the ground first. To verify this assumption we computed the apparent arrival direction of the signal energy by examining the polarization of the P-wave signal as seen on the three components of WHY. The beamformed signal direction for the earliest P-wave arrival was found to be from ~171º. The P-wave signal is propagating from the direction of the terminal detonation of the fireball (which is at an azimuth of 170° relative to WHY), confirming that the signal represents acoustically coupled body waves beginning nearly directly underneath the fireball endpoint.

Later signal arrivals in the P-wave train show energy coming from progressively more westerly azimuths. This is as would be expected presuming the shock cone intersects locations further uprange of the terminal point as time progresses and the intersection of this acoustic cone is the source for the P-waves observed at WHY.

Our final P-wave solution times and heights are relatively insensitive to slightly different values for upper crustal P-wave velocity different from the above. The effect of lower P-wave speeds (which would be the expected trend in the mountainous region near Tagish Lake) will be to push the solution to slightly larger heights. P-waves have been observed at the range of WHY from the Tagish Lake fireball trajectory (~70 km) only from the largest air-explosions (cf., Gupta and Hartenberger, 1981). P-wave signals have been reported, to our knowledge, in only two other fireball events: the Prince George fireball of 1969 (Halliday and Blackwell, 1971) and the Revelstoke meteorite fall of 1965 (Jordan and Bayer, 1967).

To further examine the question of the origin of these seismic waves, we have taken the fireball trajectory from Table 1 and modelled the expected arrival times of waves at WHY. We have used radiosonde data from WHY taken at 12 U.T. on 2000 January 18 as an input atmosphere to an altitude of 30 km and used the MSIS-E NASA atmosphere model above this height to define the acoustic velocity as a function of height. Ignoring wind corrections to this apparent sound velocity, we have computed the airwave arrivals at WHY as a function of height along the fireball path. Similarly, we compute the arrival times for P-waves, using the previously described physical model which has the airblast travelling to the ground then the induced P-waves travelling to the seismic station. A graphical version of the resulting solution is shown in Fig. 6.

A priori, ignoring fragmentation (which produces quasi-spherical symmetry along the trajectory) the ballistic-weak-shock will propagate approximately normal to the fireball trajectory (cf., ReVelle, 1976). As a result, the first arriving airwave will have as its origin that portion of the trajectory of the fireball passing closest to the station. In Fig. 6 this would be the minimum in the parabolic time propagation curve. In fact, the large-amplitude acoustic arrival occurs almost 20 s after this point.

To determine if this discrepancy is due to our ignoring of the upper winds in the calculation of the sound velocity, we have numerically modelled ray arrivals to the station from along the fireball trajectory. This simulation uses the same atmosphere as described earlier, but explicitly takes into account the wind velocity and ray propagation geometry in computing ray arrival times. As the wind velocity was very high near 30 km altitude (almost 70 m/s), this may produce significant deviations from the nominal curves, making the sound velocity a function of propagation azimuth.

The model results for propagation from various source heights are shown in Fig. 6 as solid squares. The wind effects are clearly evident (relative to the parabolic no-wind travel-time curves) and account for the timing difference. The wind is directed from an azimuth of ~300° and hence the earlier portions of the path (above 55 km altitude) have travel times decreased (being in the with-wind direction relative to WHY), while those below this height are increasingly retarded as they propagate increasingly cross-wind. Where several rays reach WHY the range in arrival times for a given height is shown. The numerical results suggest that the beginning of the main seismic signal (and the largest amplitude) is indeed from the ballistic wave propagating nearly normal to the fireball path, with significant modifications from the upper wind.

The main seismic signal beginning 208 s after the detonation continues for ~84 s. This is longer than would be expected if only the portion of the trail near the specular point were contributing the airwave signal where dispersion effects (which spread the acoustic signal in time) are minimal. Anglin and Haddon (1987) and Cumming (1989) both show examples of acoustically-coupled seismic waves from bright fireballs—in both cases, the signals persist for <10 s. In the Tagish Lake records, several additional maxima occur during this 84 s interval. While some contribution from the P-wave may be present early in the record, it is unlikely to persist for this entire interval or show such localized maxima, particularly when compared to the large amplitude surface waves. The extended signal could be a consequence of the properties of the soil proximal to the seismograph or the result of sound reflecting off the steep local terrain. No simple means of determining if extended resonance effects due to local ground properties or sound reflection are significant; we can only note that these are not seen for fireball airwaves recorded for other events by other seismic instruments at different locations.

One possible interpretation of this extended signal is that it represents acoustic energy from ongoing gross fragmentation not represented in the cylindrical blast wave model and propagating in a wider suite of directions from the fireball (ReVelle, 1976) to WHY. Such a model would suggest arrivals

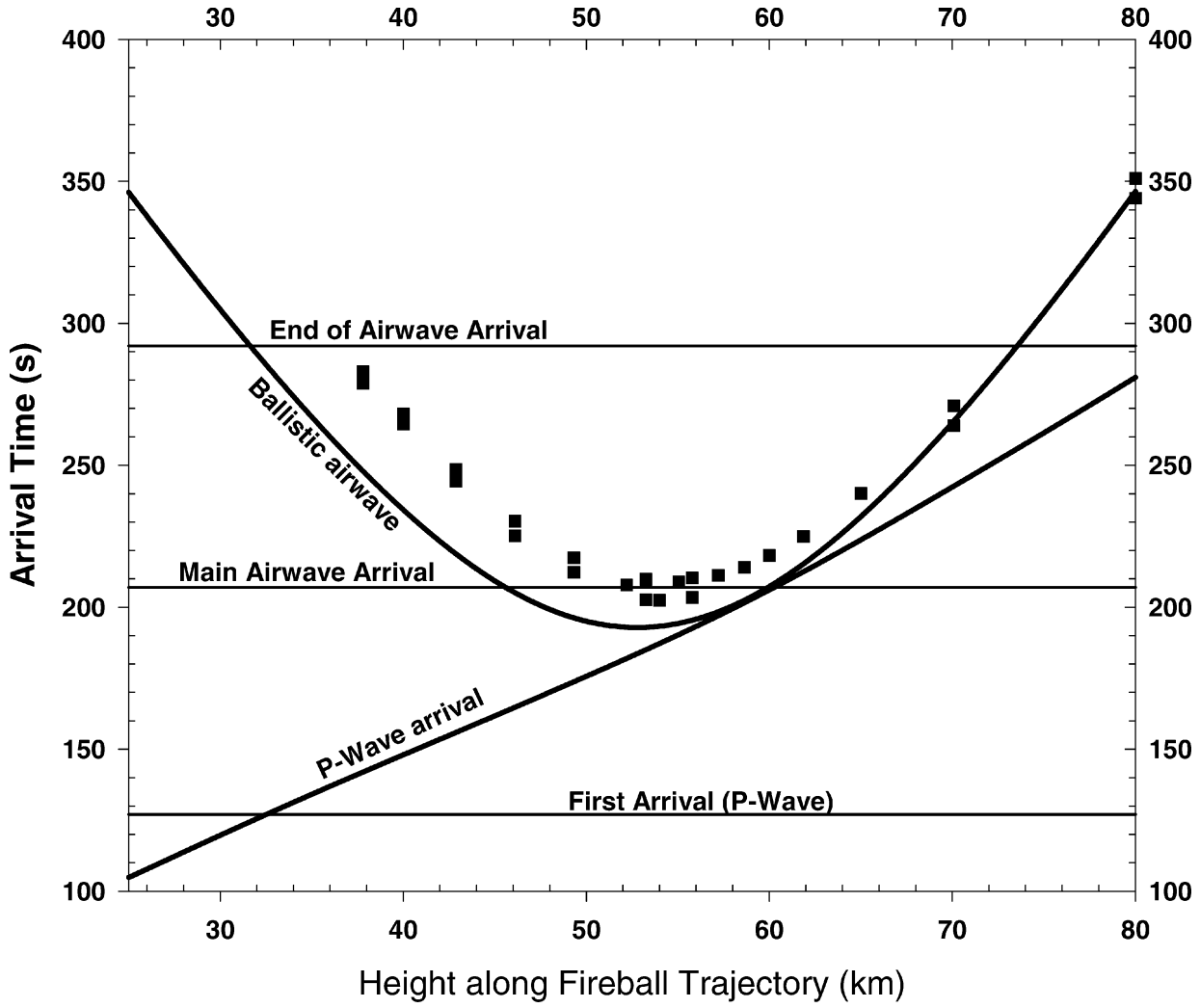

FIG. 6. Seismic wave arrival times (labelled horizontal lines) and nominal ballistic air wave arrival times at WHY using a mean sound velocity as a function of height along the fireball trajectory (parabolic line). The zero time is the time of the fireball main detonation (16:43:43 U.T.). Also shown is the solution for P-wave arrivals. Square symbols represent numerical solutions from ray-path modelling (including wind effects) at each height to WHY as described in the text. These model solutions show those heights at which acoustic ray paths to WHY exist—this does not imply actual acoustic signals arrive from such heights as this also depends on the source generation mechanism (*i.e.*, ballistic cylindrical shock *vs.* fragmentation). All modelled travel times have been corrected for the fireball's velocity.

at WHY from the terminal portions of the fireball where the satellite light curve shows significant ablation and (by inference) fragmentation. This is similar to the interpretations of Cumming (1989) and Folinsbee *et al.* (1969) where seismic data were compared to photographically determined fireball trajectories and who suggested that almost all the acoustic signal was due to acoustic energy generated near the terminal portions of the trajectory. In both cases, these locations were significantly different than the closest points along the trajectory relative to the receiving seismic stations.

Examining Fig. 6 we see that the numerical ray modelling shows acoustically accessible paths from heights along the trajectory restricted to those >37 km altitude. Our numerical modelling reveals that lower heights may produce acoustic signatures, but these are just inside the first acoustic shadow zone of the sound as seen from WHY and would not contribute significantly to the seismic signal.

That the numerical arrival times from sources near the end of the acoustically accessible trajectory end within 10 s of the cessation of the main seismic signal suggests that fragmentation along the latter portion of the path is a plausible production mechanism for the extended signal. While heights along the fireball path below 38 km will not contribute significantly to the signal, the ray modelling is a geometrical approximation which ignores scattering and diffraction effects whereby lower portions of the trajectory may contribute to some of the trailing end (last 10 s) of the main signal.

On the basis of the P-wave arrival data from WHY, we suggest that the major portion of the large-scale fragmentation for the Tagish Lake fireball ended near 32 km altitude. The

seismic solution for station HYT is shown in Fig. 7 and supports this height determination. The WHY seismic record also suggests that this fragmentation dominated the last 45–60 km (3–4 s of fireball travel through the atmosphere) of the fireball's atmospheric path in agreement with the satellite light curve which shows almost 4 s of noticeable signal (corresponding to ~60 km along the path at the nominal initial entry velocity). This suggests extensive fragmentation of the body was ongoing from 50 to 32 km altitude.

To attempt to estimate the equivalent yield energy from the seismic record requires knowledge of several uncertain parameters. We will attempt to crudely estimate these based on existing data, but caution that the final yield result is uncertain by a factor of at least several. The technique used and empirical relations derived may prove useful for future large bolide events recorded seismically.

First, the coupling efficiency of the airwave energy to production of surface waves (Rayleigh wave) is required. This is a poorly known factor with little relevant data available in the literature. For explosions in the yield range of interest, Griggs and Press (1961) quote coupling factors of 10^{-4} for surface explosions and a factor of 10^{-5} for low altitude (~10 km) airbursts. Hildebrand *et al.* (1997) found an approximate coupling factor of 10^{-7} for small bolide airbursts. For our particular source height (near 58 km) and almost certainly larger energy (compared to the bolide examined by Hildebrand *et al.*, 1997) it is unclear which is most appropriate so we choose the geometric mean of these values and adopt a coupling efficiency of 10^{-6}.

The local ground conditions greatly affect the propagation and amplitude of surface waves. Rulev (1965) showed that Rayleigh wave energies for surface explosions are greater by a factor of 10 for unconsolidated sediment (alluvium) than for consolidated (granitic rock). For the region near WHY, the rock is highly consolidated and we must include this attenuation factor in any computations.

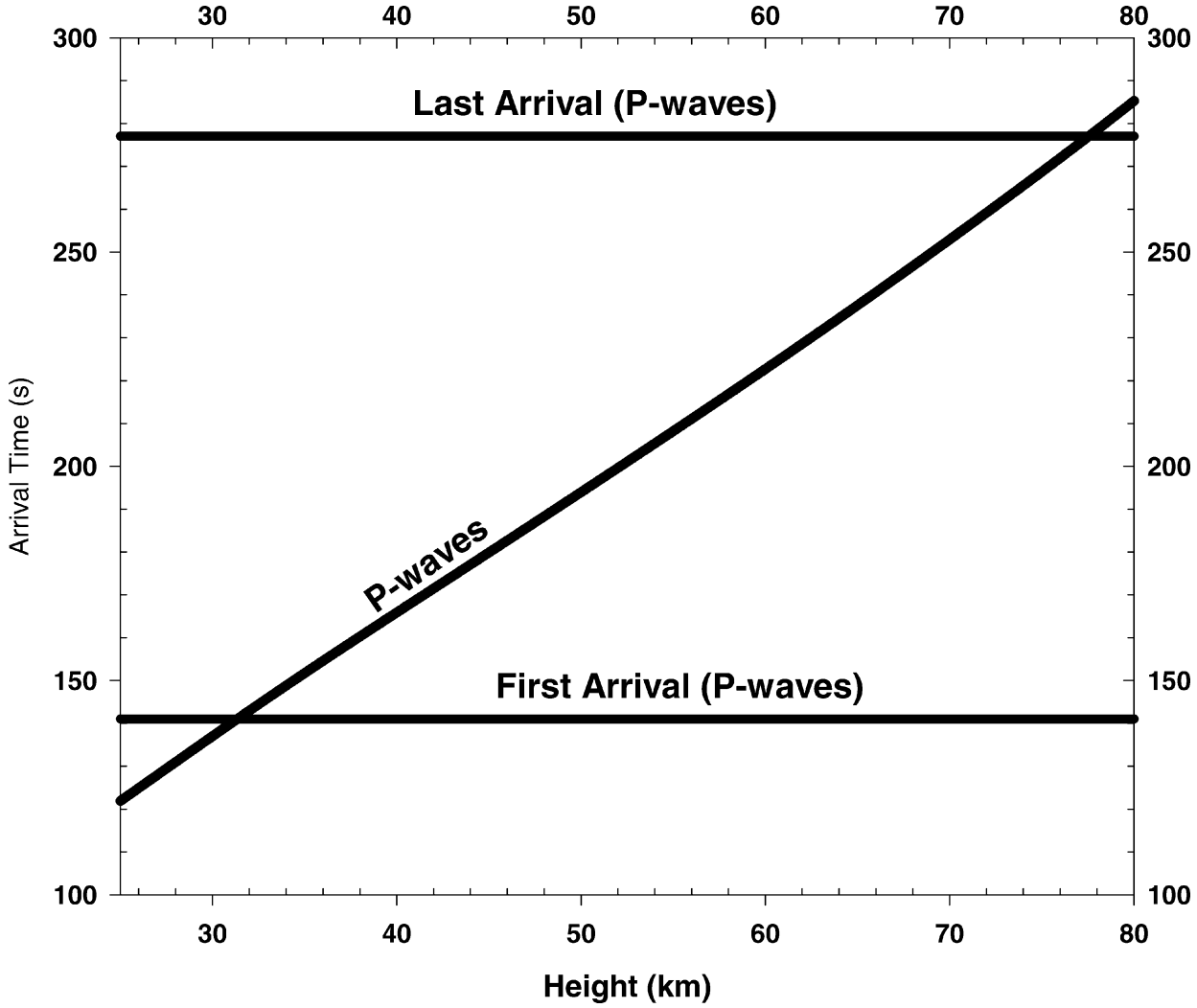

FIG. 7. Seismic P-wave arrival times (labelled horizontal lines) and expected P-wave arrivals at HYT as a function of source height along the fireball trajectory. The expected P-wave arrivals assume a near-surface P-wave velocity of 6 km/s. All modelled travel times have been corrected for the fireball's velocity.

We make use of the scaling relation found for small high-explosive surface explosions by Gupta and Hartenberger (1981) between yield, range from source and the vertical component of the peak velocity for Rayleigh waves which can be written as:

$$W = \frac{\chi R^2 (9.748 \times 10^{-11} D_v)^{1.738}}{\gamma} \quad (3)$$

where D_v is the average vertical ground motion in nm/s (zero-to-peak) over the three largest cycles of the Rayleigh wave train (corrected for the response of the seismometer), R is the range to the source in meters, W is the yield in kilotonnes of TNT equivalent energy, χ is the ratio of the air-to-ground coupling efficiency ratio for a surface explosion–airburst at altitude, and γ is the attenuation factor of the Rayleigh wave amplitude due to the composition of the local ground relative to loose soil. For Tagish Lake, the three-cycle average at the maximum of the Rayleigh wave train in the vertical component at WHY is ~800 nm/s. The range to the explosion (nearest point on the fireball path) at WHY for this earliest portion of the wave train is 63 km, which provides an equivalent surface yield (with χ = 100 and γ = 0.1) of 1.8 kT.

A summary of the estimated initial energy, mass and size of the Tagish Lake meteoroid as found by all of the previously discussed techniques is given in Table 3, together with constraints presented in H2002 based on modeling of the observed short-lived cosmogenic nuclides.

COMPARISON OF THE TAGISH LAKE FIREBALL WITH OTHER FIREBALLS

To attempt to place the Tagish Lake fireball in the context of physical data available for other fireballs, we make use of the PE criterion introduced by Ceplecha and McCrosky (1976). This statistical index is a proxy measure for the relative physical strength of a meteoroid based on the ability of the associated fireball to penetrate the atmosphere. More specifically, the PE criterion is given by:

$$PE = \log(\rho_E) - 0.42 \log m_\infty + 1.49 \log V_\infty - 1.29 \log(\cos Z_r) \quad (4)$$

where ρ_E is the air density at the fireball end-point (in units of g cm^{-3}), m_∞ is the initial mass (in grams), V_∞ is the initial velocity (in km/s), and Z_r is the zenith angle of the trajectory.

Ceplecha and McCrosky (1976), based on examination of empirical data, suggested four basic physical groupings existed in the fireball record, from the strongest, most penetrating material (group I) to the weakest material (group IIIb). These groupings have been associated with (cf., Ceplecha *et al.*, 1998) ordinary chondrites, carbonaceous chondrites, strong cometary material and weak cometary material for groups I, II, IIIa and IIIb, respectively. We emphasize that the exact PE values where one group ends and another begins is somewhat uncertain as this is a purely statistical measure. From our best estimate for the initial mass of the Tagish Lake object (see Table 3) of ~56 tonnes, its initial velocity (15.8 km/s), its known angle of entry (17.8°) and the last observed dust cloud "point" from the ground-based data of 29 km (H2002), we arrive at a PE = –5.39. This is near the border of the type II and IIIa groups (which split at PE = –5.25). Given the statistical uncertainties in the broader groups, we suggest that Tagish Lake represents the low end of the strength spectrum for carbonaceous chondrites or the very highest end of the cometary strength spectrum. This is consistent with the physical evidence from the meteorite (H2002).

A more quantitative estimate of the original Tagish Lake meteoroid physical strength can be deduced from examination of the fragmentation record of the bolide. In Fig. 1, the first local maximum in light production is interpreted as the earliest height at which fragmentation occurs. This is near 47 km altitude (using the trajectory data described in H2002) and is interpreted as the earliest clear record of large-scale fragmentation by the fireball. This is further supported by ground-based dust cloud photos which show a sequence of three small "puffs" before the main burst/extended fragmentation. The earliest of these small dust clouds occurs

TABLE 3. Summary of results for total kinetic energy, mass and equivalent radius of the Tagish Lake meteoroid derived from several techniques.*

Technique	Estimated energy (kT)	Initial mass (tonnes)	Equivalent radius (m)
Gross fragmentation model	<2.5	<97	<2.5
Porosity model	1.3–1.7	40–56 (56)	1.8–2
Infrasound	1.66 ± 0.7	33–79 (56)	1.7–2.4
Seismic	~1.7	~60	~2
Cosmogenic nuclides	2.0–2.9	65–100	2.2–2.5

*Values in parentheses are the best estimated values for the range. Cosmogenic nuclide constraints taken from Hildebrand *et al.* (2002). The initial velocity is taken as 15.8 km/s from Table 1 for the energy estimates. The equivalent radius for the pre-atmospheric body assumes a bulk density of 1.6 g cm^{-3} (from Hildebrand *et al.*, 2002).

at a height of 46 km on the fireball path, in agreement with the location established using the satellite light curve.

Figure 3 shows that the atmospheric ram pressure at the height of this first major fragmentation episode was 0.25 MPa. This is much lower than typical fragmentation pressures for meteorite-producing fireballs (Ceplecha *et al.*, 1998), but near the average for the weak fireball population. Such a low value places Tagish Lake in strength category b (the second weakest) in the system of Ceplecha *et al.* (1998). We interpret this as the minimal "global" binding strength of the larger Tagish Lake meteoroid. The ram pressure at the location of the first major burst (37 km altitude) was 0.7 MPa, and we suggest this is the most probable average binding strength for the bulk material making up the Tagish Lake meteoroid.

CONCLUSIONS

Based on the measurements of the pre-atmospheric mass for Tagish Lake from modelling, seismic, and infrasound data we estimate a best fit to these data is given by an initial mass of 56 tonnes. This corresponds to a body 4 m in diameter, using an adopted bulk density of 1.6 g cm^{-3}. From the observed satellite integrated energy, this pre-atmospheric mass, coupled with an entry velocity of 15.8 ± 0.5 km s^{-1}, results in an integral luminous efficiency value of τ_i = 16% for the Tagish Lake fireball. This is higher than has been measured for past H-chondrite falls, which have consistently yielded values near 10% (cf., Borovicka *et al.*, 2002, unpubl. data).

Application of a gross fragmentation model (assuming classical, single-body ablation) to the observed dynamics and satellite light curve result in an upper limit to the initial mass of 97 tonnes. This model breaks down for values of the ablation coefficient >0.05 s^2 km^{-2}, as a result of our simplification of a single value for the ablation coefficient for the entire flight.

A more general entry model incorporating porosity provides a better fit to the dynamics and satellite light curve for test bodies adopting the measured bulk density of the Tagish Lake meteorite. This modelling suggests the pre-atmospheric Tagish Lake meteoroid had a porosity of 37% and a mass of 56 tonnes, though values as high as 58% and as low as 37 tonnes are allowable within the constraints of the model. The best fit values from this model also suggest that 1300 kg of material reached the ground as ponderable masses. This implies that over 97% of the initial Tagish Lake meteoroid was lost to ablation.

Infrasonic records yield an energy of 1.66 ± 0.70 kT for the total energy for the Tagish Lake fireball, equating to an initial mass of 56 tonnes. The acoustic wave energy measured in the infrasound produces acoustic efficiency values for the fireball between 0.10 and 0.23%. This is comparable to the 0.14 ± 0.06% efficiency found for the Moravka meteorite-dropping fireball (Borovicka *et al.*, 2002, unpubl. data).

From the arrival times of the seismic records at WHY and HYT and the independent trajectory information derived with other techniques, the P-wave arrivals have been clearly associated with acoustic coupling of the main blast wave near the sub-terminal point. Furthermore, the airblast waves and Rayleigh wavetrains composing the major amplitude portion of the WHY record have been shown to be most consistent with a cylindrically propagating acoustic wave modified by upper level winds. The seismic record also shows evidence for numerous point-sources along the fireball trajectory which we suggest represent ongoing extensive fragmentation over the height interval 50–32 km. Without additional station information, however, this interpretation remains uncertain.

The observed fireball information results in a measure PE = –5.39, placing the Tagish Lake fireball on the periphery of the cometary fireball class. Had the Tagish Lake fireball been observed by ground-based cameras and no meteorite material recovered, it is probable it would have been classified as a cometary object. The Tagish Lake meteoroid represents the lowest strength end of the carbonaceous chondrite spectrum (as represented by type II fireballs in the classification system of Ceplecha *et al.*, 1998) or the high end of the cometary strength continuum.

The bulk compressive strength of Tagish Lake was measured to be 0.25 MPa, corresponding to the ram pressure at the height of first fragmentation. This represents the overall strength of the body limited by stress fractures, cracks and other non-uniformities. The peak dynamic pressure experienced by Tagish Lake was 1.2 MPa, though the onset of catastrophic fragmentation occurred near a ram pressure of 0.7 MPa. This latter value appears to most accurately represent the true compressive strength of Tagish Lake material.

Acknowledgements–J. Cassidy, R. Wetmiller, S. Taylor and E. Chael provided and helped interpret seismic data. D. McCormack, W. Shannon and P. Munro provided technical details for the IS10 infrasound array. Computer codes for the gross-fragmentation modelling were kindly provided by Z. Ceplecha. We gratefully acknowledge the U. S. Department of Defence for making available satellite light curve and trajectory data associated with the fireball. Funding for this research was provided by the University of Western Ontario, the University of Calgary, Sandia National Laboratories, Los Alamos National Laboratory, the National Aeronautics and Space Administration, and the Canada Research Chair Program of the Natural Sciences and Engineering Research Council. Critical review by two referees greatly improved an earlier version of this work.

Editorial handling: W. Huebner

REFERENCES

ANGLIN F. M. AND HADDON R. A. W. (1987) Meteoroid sonic shock-wave-generated seismic signals observed at a seismic array. *Nature* **328**, 607–609.

BROWN P., CEPLECHA Z., HAWKES R. L., WETHERILL G., BEECH M. AND MOSSMAN K. (1994) The orbit and atmospheric trajectory of the Peekskill meteorite from video records. *Nature* **367**, 624–626.

BROWN P. HILDEBRAND A., GREEN D. W. E., PAGE D., JACOBS C., REVELLE D., TAGLIAFERRI E., WACKER J. AND WETMILLER B. (1996) The fall of the St-Robert meteorite. *Meteorit. Planet. Sci.* **31**, 502–517.

BROWN P. *ET AL.* (2000) The fall, recovery, orbit and composition of the Tagish Lake meteorite: A new type of carbonaceous chondrite. *Science* **290**, 320–325.

CEPLECHA Z. (1996) Luminous efficiency based on photographic observations of the Lost City fireball and implications for the influx of interplanetary bodies onto Earth. *Astron. Astrophys.* **311**, 329–332.

CEPLECHA Z. AND MCCROSKY R. E. (1976) Fireball end heights—A diagnostic for the structure of meteoric material. *J. Geophys. Res*. **81**, 6257–6275.

CEPLECHA Z., SPURNY P., BOROVICKA J. AND KECLIKOVA J. (1993) Atmospheric fragmentation of meteoroids. *Astron. Astrophys*. **279**, 615–626.

CEPLECHA Z., BOROVICKA J., ELFORD W. G., REVELLE D. O., HAWKES R. L., PORUBCAN V. AND SIMEK M. (1998) Meteor phenomena and bodies. *Space Sci. Rev.* **84**, 327–471.

CUMMING G. L. (1989) Alberta Bolide of April 1, 1982: Interpretation of photographic and seismic records. *Can. J. Earth. Sci*. **26**, 1350–1355.

EWING W. M., JARDETSKY W. S. AND PRESS F. (1967) *Elastic Waves in Layered Media*. McGraw-Hill, New York, New York, USA. 380 pp.

EVERS L. AND HAAK H. (2001) Sounds from a meteor and oceanic waves. *Geophys. Res. Lett.* **28**, 41.

FOLINSBEE R. E., BAYROCK L. A., CUMMING G. L. AND SMITH D. G. W. (1969) Vilna meteorite—Camera, visual, seismic and analytic records. *J. Royal Astron. Soc. Can*. **63**, 61.

GUPTA I. N. AND HARTENBERGER R. A. (1981) Seismic phases and scaling associated with smal high-explosive surface shots. *Bull. Seis. Soc. Am*. **71**, 1731–1741.

GRIGGS D. T. AND PRESS F. (1961) Probing the Earth with nuclear explosions. *J. Geophys. Res*. **66**, 237–258.

HALLIDAY I. AND BLACKWELL A. T. (1971) The search for a large meteorite near Prince George, British Columbia. *Meteoritics* **6**, 39–47.

HALLIDAY I., BLACKWELL A. T. AND GRIFFIN A. A. (1978) The Innisfree meteorite and the Canadian camera network. *J. Royal Astron. Soc. Can*. **72**, 15.

HILDEBRAND A. R., BROWN P., WACKER J., WETMILLER R., PAGE D., GREEN D. W. E., JACOBS C., REVELLE D. O. AND TAGLIAFERRI E. (1997) The St-Robert Bolide of June 14, 1994. *J. Royal Astron. Soc. Can.* **91**, 261–275.

HILDEBRAND A. R. *ET AL.* (2002) Fall and recovery of the Tagish Lake meteorite. *Meteorit. Planet. Sci.* **37** (in press).

JORDAN J. N. AND BAYER K. C. (1967) Exploding meteor located by seismographs and microbarographs. *National Earthquake Information Bulletin* **1**.

KANAMORI H., ANDERSON D. L., MORI J. AND HEATON T. H. (1991) Seismic excitation by the space shuttle Columbia. *Nature* **349**, 781–782.

LEYA I. *ET AL.* (2001) Exposure History of the St-Robert (H5) Fall. *Meteorit. Planet. Sci.* **36**, 1479–1494.

MCCROSKY R. E. AND BOESCHENSTEIN H. (1965) The Prairie Meteorite Network. *Smithson. Astrophys. Obs. Spec. Rept.* **173**, 1–23.

OBERST J., MOLAU S., HEINLEIN D., GRITZNER C., SCHINDLER M., SPURNY P., CEPLECHA Z., RENDTEL J. AND BETLEM H. (1998) The "European Fireball Network": Current status and future prospects. *Meteorit. Planet. Sci.* **33**, 49–56.

QAMAR A. (1995) Space shuttle and meteroid (sic)—Tracking supersonic objects in the atmosphere with seismographs. *Seismol. Res. Lett.* **66**, 6–12.

REVELLE D. O. (1976) On meteor-generated infrasound. *J. Geophys. Res*. **81**, 1217.

REVELLE D. O. (1979) A quasi-simple ablation model for large meteorite entry—Theory *vs.* observations. *J. Atmos. Terr. Phys*. **41**, 453.

REVELLE D. O. (1980) Interaction of large bodies with the Earth's atmosphere. In *Solid Particles in the Solar System* (eds. I. Halliday and B. A. McIntosh), pp. 185. IAU Symposium No. **190**, D. Reidel Publ. Co., Dordrecht, The Netherlands.

REVELLE D. O. (1983) The role of porosity in modelling the dynamics, ablation and luminosity of fireballs (abstract). *Meteoritics* **18**, 386.

REVELLE D. O. (1993) The meteoroid/atmosphere interaction spectrum. In *Meteoroids and their Parent Bodies* (eds. J. Stohl and I. P. Williams), pp. 343. Proc. Intl. Astron. Symp., Astron. Institute of the Slovak Academy of Sciences, Bratislava, Slovakia.

REVELLE D. O. (1997) Historical detection of atmospheric impacts by large bolides using acoustic-gravity waves. In *Near-Earth Objects* (ed. J. L. Remo), p. 284. Annals of the New York Academy of Sciences, **822**, New York, New York, USA.

REVELLE D. O. (2001) Bolide dynamics and luminosity modeling: Comparisons between uniform bulk density and porous meteoroid models. Meteoroids 2001, Kiruna, Sweden, August 6–10, 2001.

REVELLE D. O. AND RAJAN R. S. (1979) On the luminous efficiency of meteoritic fireballs. *J. Geophys. Res.* **84**, 6255.

REVELLE D. O. AND WHITAKER R. W. (1999) Infrasonic detection of a Leonid bolide: November 17, 1998. *Meteorit. Planet. Sci.* **34**, 995–1005.

RULEV B. G. (1965) The energy in a Rayleigh surface wave from explosions in different kinds of rock. *Izvestiya* 233–241.

TAGLIAFERRI E., SPALDING R., JACOBS C., WORDEN S. P. AND ERLICH A. (1994) Detection of meteoroid impacts by optical sensors in Earth orbit. In *Hazards Due to Comets and Asteroids* (ed. T. Gehrels), pp. 199–220. Univ. Arizona Press, Tuscon, Arizona, USA.